Smart Walkers: Advanced Robotic Human Walking-Aid Systems

Anselmo Frizera Neto[1], Arlindo Elias[2], Carlos Cifuentes[1], Camilo Rodriguez[1], Teodiano Bastos[1,2], and Ricardo Carelli[3]

[1] Electrical Engineering Department, Federal University of Espirito Santo, Av. Fernando Ferrari 514, 29075-910, Brazil
[2] Biotechnology Department - RENORBIO, Federal University of Espirito Santo, Av. Fernando Ferrari 514, 29075-910, Brazil
[3] Institute of Automatics, National University of San Juan, Av. San Martin Oeste 1112, 5400, San Juan, Argentina
{anselmo,teodiano,carlos.garcia}@ele.ufes.br, arlindo.elias@ufes.br, camiloard@gmail.com, rcarelli@inaut.unsj.edu.ar

Abstract. In this book chapter, the authors present the Smart Walkers as robotic functional compensation devices for assisting mobility dysfunctions and empowering the human gait. First, general concepts of locomotion, mobility dysfunctions and assistive devices are presented. A special attention is given to the walkers, considering not only the large number of users, but mainly the rehabilitation and functional compensation potential of empowering the natural mobility. Following, robotic versions of wheeled-walkers for assisting locomotion dysfunctions are presented. In this context, the UFES Smart Walker is presented as an example of a robotic device focused on the user-machine multimodal interaction for obtaining a natural control strategy for the robotic device. Two developments are discussed: (i) an adaptive filtering strategy of the upper-body interaction forces is used in a Fuzzy-Logic based control system to generate navigation commands, and (ii) a robust inverse kinematics controller based on users-motion is presented as a new solution for controlling the Smart Walker motion. Finally, conclusions and future works in the field of walker-assisted gait is presented in the last section.

1 Introduction

1.1 Locomotion, Mobility Dysfunctions and Assistive Devices

Mobility is one of the most important human faculties and can be defined as the ability of an individual to move freely through multiple environments and perform daily personal tasks with ease [1]. Different types of pathologies, such as poliomyelitis, spinal cord injuries, multiple sclerosis or trauma, affect human mobility at different levels causing partial or total loss of such faculty. Recent evidences also show that mobility restrictions are associated to cognitive and psychosocial disturbances, which further impair the quality of life of the individual [2]. In addition, it is known that mobility decreases gradually with age as a consequence of neurological, muscular and/or osteoarticular deterioration.

S. Mohammed et al. (eds.), *Intelligent Assistive Robots*,
Springer Tracts in Advanced Robotics 106, DOI: 10.1007/978-3-319-12922-8_4

Although most gait/mobility disturbances are well recognized, only a small number of such conditions can be fully reversed by surgical procedures or rehabilitation approaches. Therapeutic alternatives in such cases include the selection and prescription of assistive devices to provide adequate functional compensation and to stop the progression of the disability and improve the overall quality of life of the affected subjects [3].

The choice of the most appropriate model of assistive device requires careful analysis and interpretation of the clinical features associated with the subject's residual motor capacity, including cognitive function, vision, vestibular function, muscle force (trunk and limbs), degenerative status of lower and upper limb joints, overall physical conditioning of the patient and also additional characteristics of the environment in which the patient lives and interacts. Severe dysfunctions in one or more of such features can compromise the safe use of the device and increase the risk of falls or energy expenditure [4].

Based on the levels of mobility restriction, the patients can be classified into two broad functional groups:

1. Individuals with total loss of the mobility capacity
2. Individuals with partial loss of mobility, presenting different levels of residual motor capacity.

Individuals belonging to the first group have completely lost the ability of move by themselves and are at high risk of confinement in bed and, consequently, to suffer the effects of prolonged immobility. Examples of subjects in this functional group include patients with complete spinal cord injury, advanced neurodegenerative pathologies, severe lower limb osteoarthritis and fractures of the spine/lower limb bones. In such cases, however, the motion can be performed by assistive technology known as alternative devices. Without the use of such equipment, the locomotion may become an impossible task for these patients, even through small spaces [5]. Some examples of alternative devices are robotic wheelchairs and special vehicles, including adapted scooters.

The mobility provided by the alternative devices can help patients to gain a certain amount of independence during daily tasks and may have positive impact on self-esteem and social interaction. However, the prolonged use of such devices do not prevent immobility-related adaptations in spine and lower limbs, characterized by loss of bone mass, circulatory disorders, pressure ulcers and other physiological impairments [6].

The second functional group is composed by individuals that present some level of residual motor capacity, which can be empowered by an assistive device. In other words, the use of such augmentative devices aims to empower the user's natural means of locomotion, taking advantage of the remaining motor capabilities. This second group of rehabilitation devices can be classified into wearable orthoses and prostheses or external devices, such as canes, crutches and walkers. In the last decade, researches in the field of intelligent augmentative devices have increased, with focus on the implementation of advanced robotic solutions for people with disability.

1.2 Walker-Assisted Ambulation: Benefits and Limitations

Conventional walkers are important examples of assistive devices because of its structural simplicity, low cost and rehabilitation potential. Walkers are usually prescribed for patients in need of gait assistance, to increase static and dynamic stability and also to provide partial body weight support during functional tasks [7]. Such devices are classified as augmentative because empower the residual motor capacity of the user, allowing a natural way of locomotion and preventing immobility-related changes. Additionally, evidence also shows that walker-assisted gait is related to important psychological benefits, including increased confidence and safety perception during ambulation.

The standard frame is the most common configuration of a passive walker, based on a metal frame with four rigid legs that must contact the ground simultaneously during each step. It is considered the most stable model, but requires a slow and controlled gait pattern, since the user must lift the device completely off the ground and move it ahead before taking a step forward [4].

Critics regarding the use of standard frames arise from evidence that shows increased force levels exerted by the upper limbs during locomotion [8]. The gait pattern imposed by the device also increases the user's energy expenditure by 217% during level walking when compared to unassisted or wheeled walker-assisted gait. Such findings restrict the prescription of standard walkers for patients presenting severe levels of metabolic, cardiac or respiratory dysfunctions [9]. Patients with cognitive disorders are also not among the scope of potential users of standard frames. This recommendation is mainly based on the results of Wright and Kemp (1992), which reported that gait assisted by standard walkers requires higher levels of attention when compared to canes or other walker models to avoid the risk of falls.

The reported adverse effects that may arise with standard frame assisted-gait suggest that the device prescription must be based on a detailed clinical assessment of the patient and the potential restrictions. To overcome such problem, other walker models were developed to provide better adaptation to the patient needs.

The two-wheeled walkers are another variation of conventional walkers. Although similar to standard frames in many aspects, these versions are characterized by the presence of two wheels mounted on the front legs (front-wheeled walkers). Such models are recommended for more active subjects or patients that have a hard time in lifting the device from the ground. The wheels allow the performance of a more natural gait pattern, but evidence shows that dynamic stability during walking is lower than standard frame assistance, and the energy expenditure is 84% higher when compared to normal ambulation [3] [4].

Rollator walkers are the evolution of the two-wheeled models and present four wheels attached to the legs of the walker. These models are faster and allow the performance of a natural gait pattern during locomotion, with lower energetic expenditure compared to other walker models. However, rollators are considered the most unstable walker version and the risk of falls is significantly increased in situations that require full body-weight support of the user, due to uncontrolled displacement of the device. In a clinical setting, rollators may be recommended for patients that require a broad walking base without the need of continuous body-weight support. The design of such models allow great number of adaptations, like braking system at the handles (to increase static stability), varied wheel sizes, robust frames, attached seat cushions, among other different gadgets [9] [3].

1.3 Smart Walkers

General Concepts. In the field of robotic technologies for gait assistance, there are several ongoing projects regarding robotic versions of canes, walkers and other guidance devices. In this context, a new category of walkers have arised, integrating robotic technology, electronics and mechanics, known as "robotic walkers", "intelligent walkers" or simply "smart walkers" [10]. Such devices present a great number of functionalities and are capable of providing mobility assistance at different functional levels, better adjusted to the individual needs of the user [11] [10].

Robotic walkers are usually mounted over a rollator framework. This configuration takes advantage of the versatility of the four wheels and the ability to maintain approximate natural patterns of walking. Stability issues are dealed with special security mechanisms to prevent falls and undesirable movement intentions from the user [11]. Several other special features can be integrated in the system, allowing the implementation of different control strategies and monitoring mechanisms.

Functional Classification of Smart Walkers. Each model of robotic walker described in the literature presents an unique set of features that complicates the classification of such systems into homogenous groups based on the overall set of functions. A classification strategy was proposed by Elias et al [11], based on the allocation of the features implemented in robotic walker systems into four functional domains (Table 1).

A review of the main robotic walker models described in the literature are provided in the following sections, in the context of each defined functional domain.

Stability and motion support. Robotic walkers are able to provide physical stability and motion support in active or passive modalities [10] [12]. In passive systems, the user has to provide the pushing energy to propel the device and the system framework tends to be lighter and simpler to assemble. It can also be equipped with several security mechanisms, like obstacle avoiding and special braking capabilities [13] [14]. Patients using this type of walker must have a postural control and walking ability [15]. Such devices are suitable for use in later stages of rehabilitation programs and domiciliary functional compensation.

Conversely, active walkers are capable of automatic propelling power and navigation, providing better control of overall motion characteristics, like speed,

Table 1. Feature-based classification of smart walkers

Classification	Functions	Features
Physical stability motion support	Propelling power Motor task assistance Motion detection	Passive Active Hybrid systems Walking Multitask assistance Force sensors
Navigation and localization components	Intelligent navigation Localization assistance	Installed maps Obstacle avoidance Environment interaction Embedded GPS Visual and voice feedback Automatic return to selected location
Biomechanical and bioelectrical monitoring	Functional monitoring Physiological monitoring	Gait and/or specific motor tasks biosignal monitoring
Safety measures	Fall prevention Emergency braking	Braking Involuntary movement detection User-device distance Gravity compensation

direction and slope negotiation [10] [12]. The device tends to be safer and suitable for patients in early stages of rehabilitation programs (lower limbs or spine surgery) or for those presenting a high degree of frailty. However, the construction of this type of walker is more complex than a passive system, and the need of extra electronic components may be reflected in higher costs [15].

Hybrid systems are also described in the literature, in which both types of control can co-exist in the device [12] [16]. This feature is especially interesting for rehabilitation purposes, since recovery protocols can be progressed from early stages, where more active control features are required, to advanced training strategies based on passive control to improve patient's proprioception and walking abilities.

Besides assisting in user's locomotion, some robotic walkers are also capable to assist other functional tasks, like sit-to-stand or stand-to-sit transfers [17] [18] [19]. The versatility of these multifunctional systems may have a positive impact in several clinical scenarios where upright postural training or stimulation are needed, such as inpatient rehabilitation following orthopaedical surgical procedures, elderly with poor postural control or lower limb weakness and patients presenting pathological gait patterns.

Several models of robotic walkers are equipped with force sensors in the handles of the device [20]. Such sensors are used to detect the subject's intents of movement, and it enhances the cognitive human-machine interaction. Force signals are converted into guidance commands through filtering and classification strategies [21]. In addition, involuntary movements of the user can also be detected and classified, avoiding undesirable motion commands.

An innovative forearm support was developed for the Simbiosis walker which was also used to detect force interactions patterns during motion level walking and to identify user's intent of movement [10] [21]. The detection of force patterns, both in handles or alternative supports, can also be used to identify altered gait patterns that can be corrected by a feedback intervention by the physical therapist.

Navigation and Localization Components. Navigation systems are a common feature of robotic walkers. The main objective of such hardware is to increase locomotion safety, since the embedded sensors are able to detect and automatically avoid obstacles, negociate an alternative route and also notify the user about the shape and location of the obstacle. This feature is of special interest for people with severe visual disturbances [22] [23] and may act in conjunction with active systems to drive the user safely throughout a closed environment.

This function can be accomplished by previous knowledge of the environment's map [23], or by real time obstacle detection and negotiation [24]. The first mode is suitable for closed environments, such as homes or clinical scenarios. The later mode is indicated for open or dynamic environments, being suitable for patients with more active lifestyle. In either way, these features may give more confidence to the patient in early stages of rehabilitation programs, and gait training can be safely done in either ambulatory or hospital settings, or even at home.

The devices can also communicate with the user via visual or voice feedbacks, informing the presence of obstacles and giving direction options [12] [23].

Autonomous localization features are relevant for patients with cognitive disturbance, sensory degradation and loss of memory that are associated with neuro-degenerative diseases such as Alzheimer or Parkinson. GPS devices can be installed in robotic walkers in order to keep track of the patient in a particular environment or outsides [10].

Modern systems are also able to interact with specific sensors in the environment, supplying the patient with direction options and localization via visual feedback [25].

Biomechanical and Bioelectrical Monitoring. Besides movement and navigation assistance, smart walkers present monitoring features that are of significant relevance for rehabilitation programs. Recent studies investigating gait parameters detected by smart walkers have shown the potential and versatility of this type of assistive device in treatment planning and progression. This feature also adds the possibility of out-of-the-clinic monitoring.

In a clinical setting, several gait parameters can be monitored by therapists in a treatment session using robotic walkers, including speed of movement, total distance traveled, gait patterns, total amount of force/torque exerted in the handles during gait, movement acceleration/deceleration, stride to stride distance and several others [26] [27] [28] [29] [30].

The detection of dysfunctional gait patterns during training sessions with smart walkers can provide additional clinical data that can be used by the clinician to improve the overall treatment program and progression, which can reflect in increased precision and quality of the intervention.

In addition to biomechanical and bioelectrical data analysis acquisition, the monitoring of other physiological signals through smart walkers is also possible and can be used to keep track of associated co-morbidities of the user. The PAMM system, developed by MIT, was the first to present an embedded electrocardiogram monitor system. Modern walkers are also able to monitor blood oxygenation through photoplethysmography sensor located in the handles of the device [27] [28].

All this information can be used to record a medical and/or functional history of the user and can also be sent via a remote terminal to the professional staff responsible for the rehabilitation program [10] [29] [31].

Safety Measures. Safety is a major concern of robotic walker systems, since the user must rely on the support provided by the device to perform the necessary tasks of rehabilitation programs or daily activities.

Several strategies to prevent falls and to help stabilize the user's gait pattern are described in the literature. The main features associated with such function are emergency braking capabilities, jerky movement detection, gravity compensation and user-walker distance monitoring.

Emergency braking are often associated with obstacles and stairs detections, acting together with navigation components [14] [15] [24]. Gravity compensation is another feature that makes use of intelligent navigation, allowing the recognition and proper negotiation of terrain irregularities, such as slopes [15].

Irregular or jerky movements are indicative of postural imbalance and can be detected by force sensors in either handles or forearm support [10], braking the device to provide enough support for postural recovery [21].

A remarkable feature of some systems is related to the placement of rear sensors in the device. The objective is the constant monitoring of the distance between the user and the walker. Increasing of this distance is detected by the rear sensor and, thus, emergency braking is performed, allowing the user to re-establish the correct, and safer, distance [14]. A recent model presented an innovative step-by-step technology that enabled the walker to keep the same pace of the user by monitoring the user's footsteps [12].

Braking the device is also important to provide support for sit-to-stand and stand-to-sit assistance, avoiding slipping or undesired movement of the walker that could increase the chance of falls [15] [23].

Following, the full development of the UFES Smart Walker, a robotic system built at Federal University of Espirito Santo, is presented to illustrate the main features and rehabilitation potentials of such assistive devices.

2 UFES Smart Walker. System Overview

In this section, the UFES Smart Walker is presented (Fig. 1). The device focuses on enhancing safety and stability during assisted gait by means of partial body

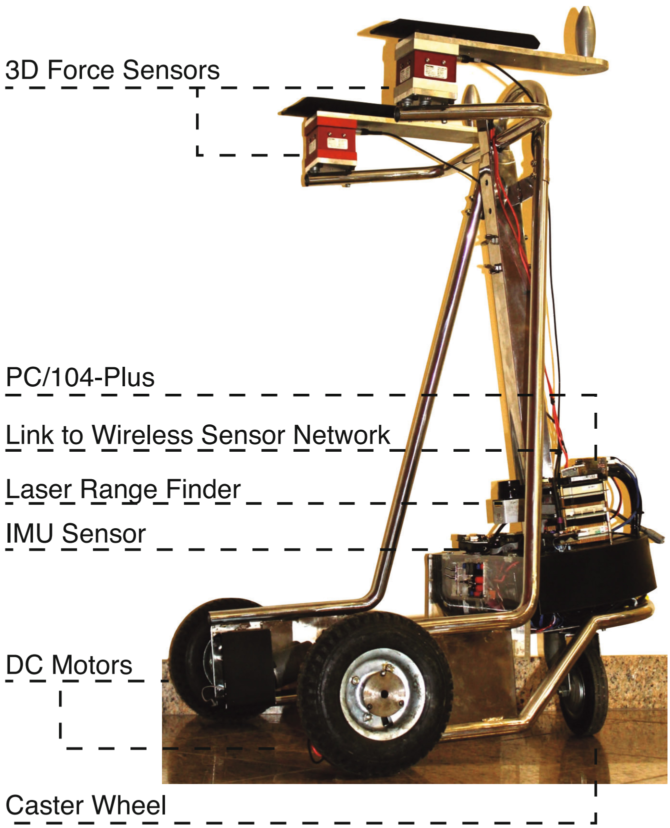

Fig. 1. The UFES Smart Walker and its subsystems

weight support and the use of advanced control strategies. The control system relies on a human machine interface (HMI) responsible for the acquisition and interpretation of user's postures and gestures during gait. Both upper and lower limbs information are combined in order to command the device's motion.

The robotic walker developed under the framework of the research project presents three sensor subsystems designed for the acquisition of gait parameters and for the characterization of the human-robot interaction during gait. First, the *upper-body force interaction subsystem* is based on two tridimensional force sensors (Futek MTA400) installed under the forearm supporting platforms. The forces signal acquisition is performed by an acquisition module installed on the embedded computer described below.

The second subsystem is based on a laser range finder (LRF) sensor (Hokuyo URG-04LX) to measure the user's feet evolution during the assisted gait. The LRF sensor is mounted on the walker framework at the legs height and the legs location is estimated in real-time by means of a processing board based on the

Microchip dsPIC33F micro-controller. A full scan, which provides the position of each leg, is performed by the laser sensor every 100 ms.

Finally, wireless inertial measurement units (IMU), developed in previous research project [32], are integrated into the system architecture. One of them is installed in the walker's structure, as shown in Fig. 1. Other IMUs can be integrated into the real-time architecture by means of the wireless link for biomechanical monitoring and to provide kinematic information to be used in the control strategies. All IMUs are linked using ZigBee protocol setting up a wireless sensor network that communicate via serial interface with the embedded computer. In the application presented in this chapter (see section 3.2), the IMU information is used to get walker and human orientation and human angular velocity to provide information to the controllers. IMU information is sampled every 20 ms.

An embedded computer based on the PC/104-Plus standard performs control and processing tasks and integrates the previously presented subsystems. It is based on a 1.67 GHz Atom N450, 2 GB of flash memory and 2 GB of RAM. The application is integrated into a real-time architecture based on Matlab Real-Time xPC Target. A laptop computer is used for programming the real-time system and to save the data from the experiments. It is connected to the PC/104-Plus by UDP protocol. If data recording is not necessary, the robotic system is able to operate without the laptop computer.

Fig. 1 summarizes the system architecture and subsystems installed on the walker's structure.

Regarding the feature-based classification of smart walkers, the UFES Smart Walker integrates functions related to:

- Physical stability and motion support. The device integrates forearm supporting platforms to allow partial body weight support. Additionally, the traction motors installed on the device's rear wheels offer an assistance to the propelling power. Finally, the sensors subsystems are also used for extracting the user's navigation intentions.

- Biomechanical monitoring. As it will be presented in section 3.2, gait parameters, such as cadence and step length, can be extracted by combining the data obtained from the LRF and IMU sensors. By using additional IMU sensors placed on the user's lower limbs, joint kinematics can also be measured.

- Safety measures. Considering the safety measures, a set of rules regarding the interaction forces and user-walker distance parameters are integrated into the device control architecture (see section 3.1). Emergency braking is performed in the case of unsafe situations. Involuntary interaction forces are also canceled in real-time during the operation of the device. The DC motors used for traction also automatically brake in cases of power failure or overheating of the motor electronic drivers.

3 Development of Controllers Based on User-Machine Interaction During Assisted Gait

In this section, two control strategies are presented. First, in section 3.1, an adaptive filtering strategy of the upper-body interaction forces is fed into a Fuzzy-Logic based controller. Section 3.2 addresses a robust inverse kinematics controller in which the navigation commands are obtained from the user's motion measured using the laser range finder and the inertial measurement units.

3.1 Adaptive Filtering of Force Interaction for the Identification of Guidance Intentions

On a previous research project that was the framework to the development of the Simbiosis Walker [33], a study regarding the force interaction during assisted gait led to the identification of three main components. The typical force data acquired on the y axis (F_y in Fig. 2) of one of the force sensors is presented in Fig. 3.

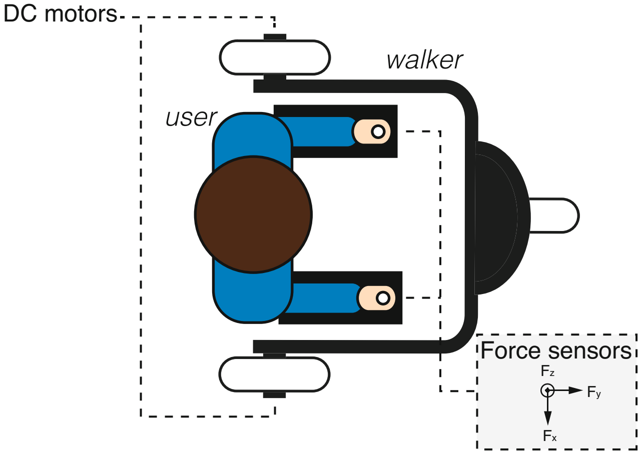

Fig. 2. The human-walker model used for the force interaction controller

The high frequency component is caused by the vibrations introduced by the floor/walker wheels imperfections and should be eliminated. The second component is due to the oscillations of the user's trunk during gait. This second component contains important information related to the user's gait (cadence, heel-strike and toe-off instants) and the evolution of the center of gravity (CoG) during the locomotion [34]. Nevertheless, this component does not reflect the user's locomotion intentions and, therefore, should be filtered. Finally, the voluntary components related to the user's navigational commands are the focus of interest in this approach.

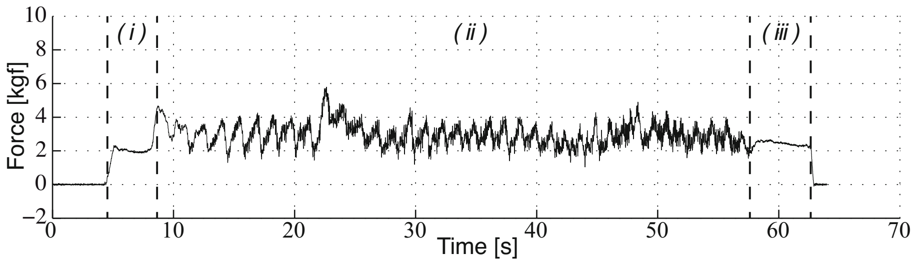

Fig. 3. Typical force signal (y axis) obtained experimentally. Areas (i) and (iii) indicate the periods that the user is supported by the device and is not walking. Area (ii) indicate the walking part of a sample experiment.

These voluntary components are also found within the force sensor data presented in Fig. 3 and can be seen as transient components that must be properly extracted in order to generate commands that drive the walker's motion.

The presence of the three force components led to the development of a technique for obtaining and characterizing such components in order to extract the user's commands to control the device [35]. This filtering technique will be addressed in the following sections.

Cancellation of the Vibrations Components Introduced by Floor/ Walker Wheels Imperfections. Irregularities on the ground or imperfections on the device's wheels cause mechanical vibrations in higher frequencies, where no gait or user's commands components are found. Classical low-pass filters can be generally used for the cancellation of high-frequency components of the force signals. Nevertheless, such approach would also introduce an important phase shift between input and outputs signals causing a temporal delay on the filtered signal. Such situation is undesirable in real-time applications once delay can affect the natural interaction between both agents (walker and user).

Therefore, to avoid the undesirable delays and considering the nature of the vibration signals, a filtering strategy with prediction would be a suitable approach. Architectures based on particle filters or Kalman algorithms could be an good alternative for such situations, but their use can imply in higher computational cost.

To overcome such limitation, a filtering architecture for the cancellation of such vibration components based on *g–h filters* was chosen. G–h filters are simple recursive filters that estimate future position and velocity of a variable based on first order model of the process. Measurements are used to correct these predictions, minimizing the estimation error.

G–h filters are closely related to Kalman filters and to linear state observers, but can be seen as a simpler approach as they do not require a detailed system model. Kalman filtering requires the time-dependent estimate of the state covariance to be updated automatically, in order to calculate the Kalman gain matrix terms. G–h filters gains, alternatively, are manually selected and (usually) static.

Traditional applications of g–h filters are radar tracking and aeronautics [36]. The general form of a g–h filter is described in equations (1), (2), (4) and (5).

Equations 1 and 2 are known as update equations. These equations provide an updated estimate of the present target position and velocity based on the present measurement of target position (y_k) as well as on prior measurements. These equations are also called the filtering equations. Confidence on measures is weighted by the gains g_k and h_k.

Thus, $x^*_{k,k}$ is called the *filtered estimate* of x_k at the present time based on the use of the present measurement (y_k) and the past measurements. $x^*_{k,k-1}$ is the *prediction estimate* of x_k based on past measurements.

$$x^*_{k,k} = x^*_{k,k-1} + g_k(y_k - x^*_{k,k-1}) \tag{1}$$

$$\dot{x^*}_{k,k} = \dot{x^*}_{k,k-1} + \frac{h_k}{T_s}(y_k - x^*_{k,k-1}) \tag{2}$$

$$\tag{3}$$

Equations 4 and 5, or prediction equations, provide a prediction of future position and velocity, $x^*_{k+1,k}$, $\dot{x^*}_{k+1,k}$, based on the first order dynamic model of the variable. Thus, these equations allow to predict what the target position and velocity will be at the time $k+1$ and to repeat the entire update process previously described in equations (1) and (2). As it can be observed, $x^*_{k+1,k}$ and $\dot{x^*}_{k+1,k}$ are calculated with the filtered estimate of the current position and velocity ($x^*_{k,k}$ and $\dot{x^*}_{k,k}$, respectively).

As g–h trackers consider a constant velocity model, the predicted velocity $\dot{x^*}_{k+1,k}$ is equal to the current one, $\dot{x^*}_{k,k}$.

$$x^*_{k+1,k} = x^*_{k,k} + T_s\dot{x^*}_{k,k} \tag{4}$$

$$\dot{x^*}_{k+1,k} = \dot{x^*}_{k,k} \tag{5}$$

The assumption of constant speed is reasonable in the proposed application, considering that human movements are slow and present small accelerations [37], especially taking into account that data are sampled at much higher rates ($f_{sampling} = 1kHz$ for this study).

It is also possible to combine equation (1) with (4) and equation (2) with (5) to obtain the *g–h prediction-filtering equations* presented in equations 6 and 7.

$$x^*_{k+1,k} = x^*_{k,k-1} + T_s\dot{x^*}_{k+1,k} + g_k(y_k - x^*_{k,k-1}) \tag{6}$$

$$\dot{x^*}_{k+1,k} = \dot{x^*}_{k,k-1} + \frac{h_k}{T_s}(y_k - x^*_{k,k-1}) \tag{7}$$

Tuning g–h filters consists of selecting appropriate values for g_k and h_k. Thus, an important class of g–h filters are those for which g and h are fixed, as the computations required for processing are very simple, [36]. This is especially important in the proposed robotic application, considering that it consists on a embedded real-time system.

From previous experience [35], the Benedict-Bordner Filter (BBF), an approach for selecting the values of g_k and h_k, presented excellent results. BBF minimizes the total transient error, defined as the weighted sum of the total transient error and the variance of prediction error due to measurement noise errors [38]. BBF is the constant g-h filter that satisfies:

$$h = \frac{g^2}{2 - g} \tag{8}$$

As g and h are related by Equation 8, the BBF approach has only one degree of freedom. Additionally, g_k and h_k are constant (g and h), which implies a great simplification on the filtering architecture. Fig. 4 presents an example of a force signal filtered with the proposed technique.

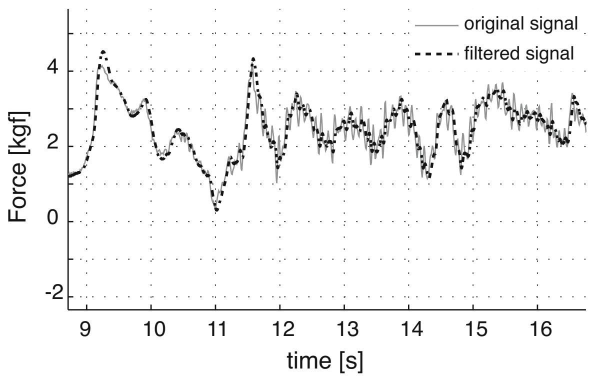

Fig. 4. Result of the filtering architecture for the cancellation of vibrations components introduced by floor or walker wheels imperfections

Estimation of Gait-Related Force Components and Extraction of Navigation Commands. This section presents a methodology for the estimation of the force component related to the user's gait. As previously commented, this component occurs due to the motion of the user's trunk during gait, which causes an oscillatory behavior on the measured forces.

For that purpose, taking advantage of the periodicity of the signals and its close relation with the gait cadence, an adaptive filter based on the *Fourier Linear Combiner* (FLC) was chosen for this filtering stage.

It is important to mention that the frequency of the gait related force components is very close to the voluntary components that contain the user's commands. This way, the use of low pass filtering could eliminate the voluntary components and, therefore, jeopardizing the proper functioning of a natural interaction.

FLC is an adaptive algorithm used for continuous estimation of quasi-periodical signals based on a M harmonics dynamic Fourier model (Equation 9). Using frequency and the number of harmonics as inputs for the model, the algorithm adapts amplitude and phase for each harmonic at the given frequency.

$$s = \sum_{r=1}^{M} [w_r sin(r\omega_0 k) + w_{r+M} cos(r\omega_0 k)] \tag{9}$$

The adaptation of the coefficients w_k is performed based on the least-mean-square (LMS) recursion, a descend method based on a special estimate of the gradient [39], which ensures inherent zero phase. The equations for the FLC algorithm are described below.

$$x_{r_k} = \begin{cases} \sin(r\omega_0 k), & 1 \leq r \leq M \\ \cos((r-M)\omega_0 k), & M+1 \leq r \leq 2M \end{cases} \tag{10}$$

$$\varepsilon_k = y_k - \mathbf{W}_k^{\mathrm{T}} \mathbf{X}_k \tag{11}$$

$$\mathbf{W}_{k+1} = \mathbf{W}_k + 2\mu\varepsilon_k \mathbf{X}_k, \tag{12}$$

where:

- y_k is the input signal;
- $\mathbf{W}_k$ is the adaptive weight vector that generates a linear combination of the harmonic orthogonal sinusoidal components of the reference input vector;
- $\mathbf{X}_k$ is the reference input vector;
- M is the number of the harmonics used in the model;
- μ represents the amplitude adaptation gain used for the LMS recursion.

As mentioned before, the FLC algorithm needs a frequency input for the correct estimation of the gait related force component. This frequency information is the gait cadence that is directly obtained by the laser range finder (LRF) sensor that measures the user's feet evolution during assisted gait.

Fig. 5 shows the complete filtering scheme for obtaining the user's navigation commands and the effect of the filtering architecture in a sample force signal. The filtered force signals (red line in Fig. 5) contain the user's navigation commands and serve as input signals to the controller presented in the following section.

Identification of User's Commands and Fuzzy-Logic Controller. The control strategy based on force interactions is presented in Fig. 6. The force signals filtered with the presented algorithm were used to drive the walker's motors through a controller based on fuzzy logic. y and z force components (see Fig. 1) from right and left sensors are filtered individually using the filtering architecture previously presented (Fig. 5).

F_y components are divided by the F_z components (when $F_y \neq 0$) in order to obtain force signals that are proportional to the amount of body weight applied in each armrest. This operation corrects asymmetrical supports caused by an

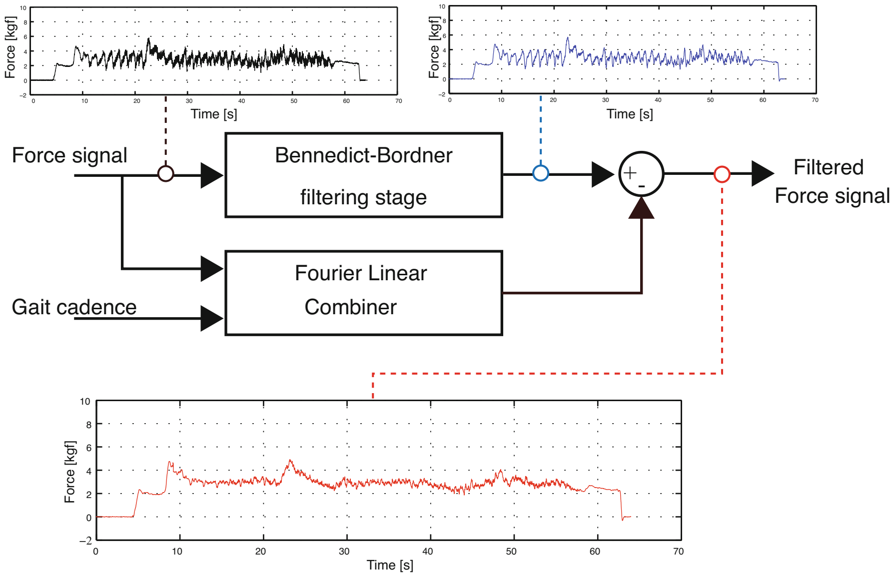

Fig. 5. Filtering architecture and the effects on a sample force signal

unilateral affection on the gait. Then, signals are conditioned to input the fuzzy logic classifier. The conditioning process consists of applying a *gain*, to adjust to the correct range of inputs; a *saturation function*, to avoid values over the input limits of the fuzzy classifier; and a *dead-zone*, to prevent motor commands in cases of signals very close to zero and, thus, not high enough to move the device.

The main element of the control scheme (Fig. 6) is the fuzzy logic block. It is built upon the information obtained experimentally from the tests performed with healthy subjects. It combines information of right and left sensors to generate motor commands. The filtered and conditioned force signal inputs can vary from -1 to $+1$ and are grouped into four classes:

– *Negative*, *Z-shaped* function with $a = -0.8$ and $b = 0$, Equation (13).

$$zmf(x) = \begin{cases} 1, x \leq a \\ 1 - 2 \cdot (\frac{x-a}{b-a})^2, a \leq x \leq \frac{a+b}{2} \\ 2 \cdot (b - \frac{x}{b-a})^2, \frac{a+b}{2} \leq x \leq b \\ 0, x \geq b \end{cases} \tag{13}$$

– *Zero*, Gaussian symmetrical function with $\sigma = 0.2045$ and $c = 0$, Equation (14).

$$gaussmf(x) = e^{\frac{-(x-c)^2}{2\sigma^2}} \tag{14}$$

– $Positive_{low}$, Gaussian symmetrical function with $\sigma = 0.1173$ and $c = 0.4$.
– $Positive_{high}$, *S-shaped* function with $a = 0.3148$ and $b = 0.8$, Equation (15).

$$smf(x) = \frac{1}{1 + e^{-a(x-b)}} \tag{15}$$

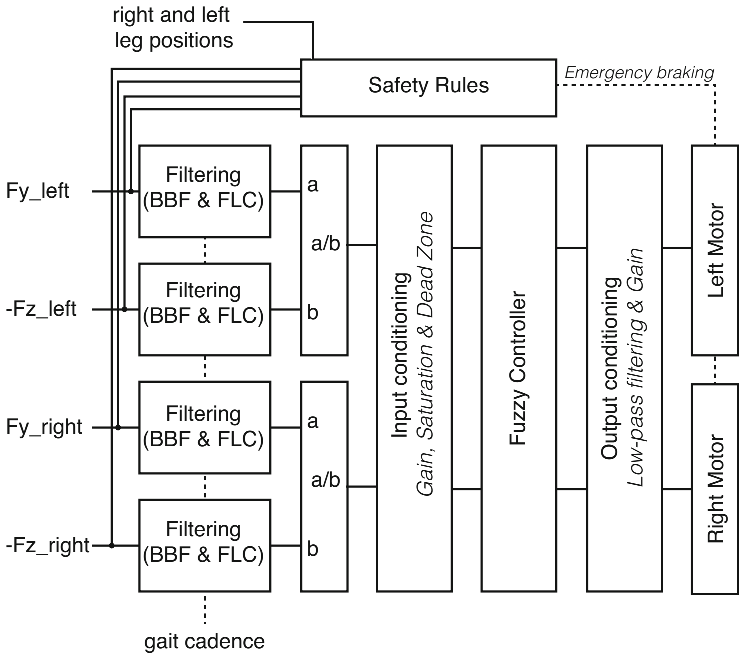

Fig. 6. Control strategy based on the user-walker interaction forces

Three functions were defined to the outputs:

- *Zero*, *Z-shaped* function with $a = -0.2$ and $b = 0.5$.
- $Positive_{low}$, Gaussian symmetrical function with $\sigma = 0.1944$ and $c = 0.5$.
- $Positive_{high}$, *S-shaped* function with $a = 0.5$ and $b = 0.8$.

A set of sixteen rules were implemented in the fuzzy logic architecture as presented in [40].

After the fuzzy logic block, the signals are passed through the output conditioning block that performs two functions: (i) low pass filtering to avoid eventual abrupt changes in control signals and, thus, ensuring comfortable navigation to the user; and (ii) signal adjustments (offset corrections and gains) to the analog range of inputs of the motor control board.

It is important to mention that, due to safety reasons, no backward motion was allowed. This will be implemented in the future and will only be active in special situations determined by the patient's needs.

Finally and also regarding safe navigation, it is important to mention that some safety rules were implemented into the system. These are simple rules that automatically brake the device's motors, presenting the highest priority in the control scheme. The UFES Smart Walker automatically brakes if:

- If both F_y components are negative (the system associates this with the intention to brake),

- If any of the F_z components is smaller than a certain value (forearm not placed on the armrests),
- If there is an excessive separation between user's legs and the device (user is left behind),
- If there is not enough separation between the user's legs and the device (user too close with not enough space to walk).

Under normal operation, none of these rules are activated and the proposed control scheme acts on the device's DC motors.

The developed filtering and control strategy were implemented into the device's firmware and the system was taken for clinical validation as it is discussed in the following section.

Results and Discussion. This first implementation of the control strategy is similar to the one integrated in a preceding research project that originated the Simbiosis Walker [33]. This section presents a short description of the clinical validation of the control scheme at the Biomechanical Unit of Spinal Cord Injury Hospital of Toledo (HNPT).

The trial experimentation consisted of walking in a U-shaped track, from point 1 to point 2 and back to point 1, as presented in Fig. 7. No instructions or training were provided in order to prepare the subjects for the proposed task and no adjustments of the controller was performed to adjust the device to the subject. The authors suggested that if the proposed interface and interaction strategy are supposed to be natural, no training should be required.

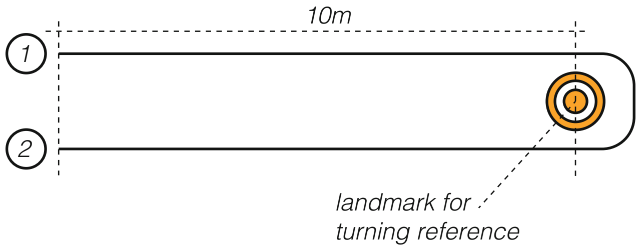

Fig. 7. U-shaped track used in the clinical validation of the control strategy

A total number of eight (incomplete spinal cord injury) patients were selected by the clinical staff taking into consideration inclusion factors such as: preserved cognitive functions, capacity of maintaining a standing position, capacity of grasping and being able to walk with or without the assistance of an assistive device.

The subjects were fitted into three subcategories:

- Two subjects presented severe impairment of the locomotion system. The objective here is to observe if the control scheme can be used in rehabilitation

scenarios. Notice that the subjects use almost exclusively wheelchairs as their assistive devices.
- Four patients that use the wheelchair as their main locomotion assistance, but can walk for short periods of time with the assistance of a device. The most common complain in this case is that existent technical aids do not provide a satisfactory experience and the risks of fall are important, causing the subject (or therapist) to choose the wheelchair as a safety measure. The aim is to evaluate the developed system as a functional compensation device.
- Two patients with the least affections in gait. Both of them were users of conventional two-wheeled walker at some point in their rehabilitation process. This small group can offer important feedback and comparison of the developed strategy versus the use of conventional / passive walkers.

All patients were able to use the device and walk the proposed track with self selected speed. The adaptive filtering scheme provided a mean amplitude cancellation of 73.18% of the cadence related force components and fuzzy logic control strategy offered smooth and responsive navigation. Fig. 8 shows an example of raw and filtered F_y signals and the velocity signal of the motorized wheels during a sample experiment.

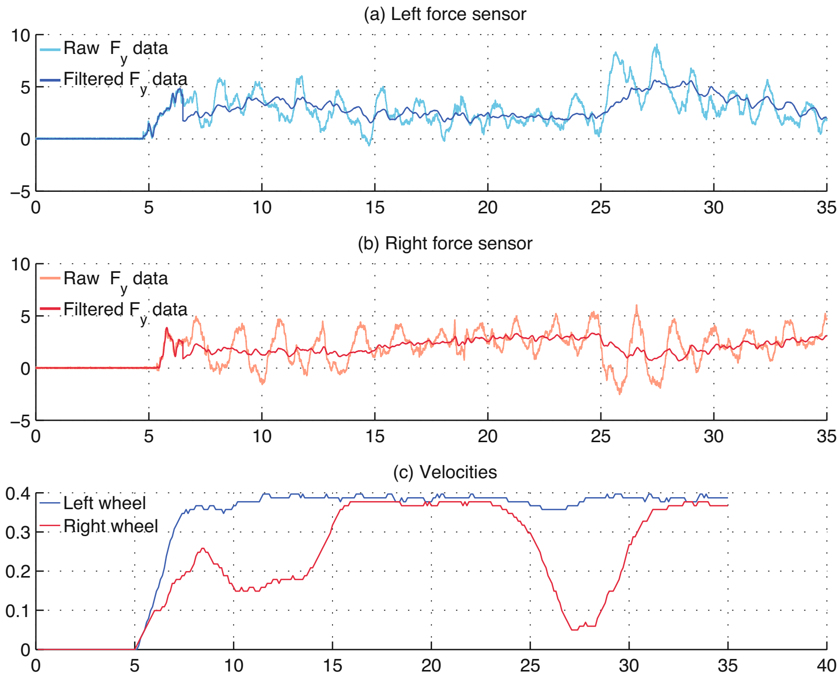

Fig. 8. Sample of clinical validation data: (a) raw and filtered left F_y data; (b) raw and filtered right F_y data; and (c) left and right wheel velocities

3.2 Inverse Kinematics Controller Based on Feet Evolution

The filtering and control strategy presented in the previous section showed good results in the clinical validation, assisting the user's gait at the same time that partial body weight support was performed. Information obtained from the laser range finder (LRF) was only used in order to provide cadence information and, therefore, the subsystem was not used to its full potential. Additionally, the inertial measurement unit (IMU) placed on the user's pelvis could provide important insights regarding the user's intentions and locomotion commands.

This section presents an implementation of a multimodal interaction scheme to be used in a control strategy for walker-assisted locomotion, using a LRF for tracking the human legs, and an IMU for capturing the human movement during the gait.

Proposal of Control Strategy. The human-walker interaction model is shown in Fig. 9. The variables and parameters used in the presented model are: human linear velocity (v_h), human angular velocity (ω_h), human orientation (ψ_h), walker linear velocity (v_w), walker angular velocity (ω_w) and walker orientation (ψ_w). The interaction parameters were defined as the angle ϕ between v_h and $\overline{WH}$ (named Human-Walker Line), the angle θ between $\overline{WH}$ and $\overline{WC}$ segments, and d, the length of $\overline{WH}$. Finally, the parameter a defines the distance between the controller reference point (W) and the walker center of rotation (C).

The control proposal is based on the inverse kinematics and the control variables are the angle ϕ and the distance d. The control law of this system aims to achieve a desired human-walker distance ($d = d_d$) and a ϕ angle that con-

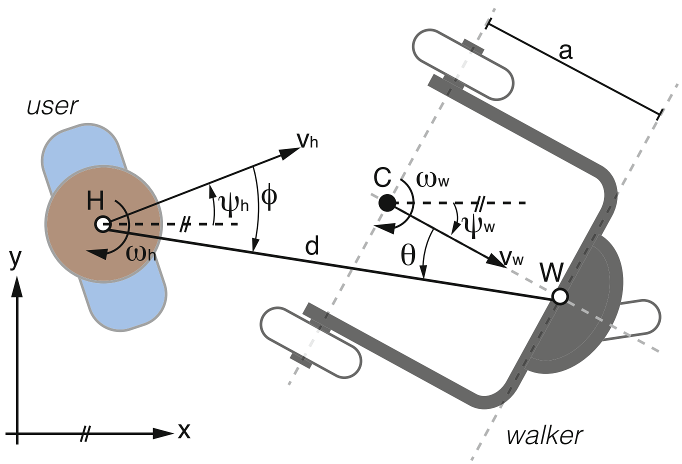

Fig. 9. The human-walker interaction model used for the inverse kinematics controller

verges asymptotically to zero. Direct kinematics is shown in (16), where $\tilde{d}$ is the difference between the desired and measured distances.

$$\begin{pmatrix} \dot{\tilde{d}} \\ \dot{\tilde{\phi}} \end{pmatrix} = \begin{pmatrix} \cos(\theta) & -a\sin(\theta) \\ -\frac{\sin(\theta)}{d} & -a\frac{\cos(\theta)}{d} \end{pmatrix} \overbrace{\begin{pmatrix} v_w \\ \omega_w \end{pmatrix}}^{u} + \begin{pmatrix} -v_h\cos(\phi) \\ \omega_h + v_h\frac{sin\phi}{d} \end{pmatrix} \tag{16}$$

The inverse kinematics controller, obtained from the kinematic model presented in (16), is shown in (17) and (18).

$$v_w = \cos(\theta)\ \left[-k_d\tilde{d} + v_h\cos(\phi)\ \right] - dsin(\theta)\left[-k_\phi\tilde{\phi} - \omega_h - \frac{v_h}{d}\sin(\phi)\ \right] \tag{17}$$

$$\omega_w = -\frac{\sin(\theta)}{d}\left[-k_d\tilde{d} + v_h\cos(\phi)\ \right] - \frac{d}{a}\cos(\theta)\ \left[-k_\phi\tilde{\phi} - \omega_h - \frac{v_h}{d}\sin(\phi)\ \right] \tag{18}$$

It could be demonstrated that the control system is exponentially and asymptotically stable, thus obtaining (19) and (20).

$$\tilde{d}(t) = \tilde{d}(0)\,e^{-k_d t} \tag{19}$$

$$\tilde{\phi}(t) = \tilde{\phi}(0)\,e^{-k_\phi t} \tag{20}$$

The proposed control strategy was simulated with different human locomotion patterns (straight lines, circle-shaped paths, eight-shaped paths, etc.) in order to observe whether the walker correctly follows the user. Fig. 10 shows one of the proposed simulations in which the human path performing an eight-shape curve (input) and the walker path following the human in front (controller output) are shown. Distance and angular errors are also kept withing low values. Therefore, the proposed controller is expected to keep the walker continuously following the human during gait while maintaining itself positioned in front of the user.

As the system architecture is based on Matlab Real-Time xPC Target, the implemented equations used for the simulations can be directly applied to the walker control architecture, avoiding the possibility of implementation errors.

It is possible to state that a good real-time implementation of the method proposed in this section relies on robust and precise measurement or estimation of the parameters used in the control scheme (see equations 17 and 18). This way, the next sections present the methods used to obtain all these parameters in real-time along with the experimentation, results and discussions of the proposed control proposal.

Estimation of Interaction Parameters. As previously discussed, the quality of the control approach relies on the correct estimation of the interaction parameters. Such parameters represent the link between the user and the walker in the control strategy. The method to obtain the parameters of the proposed model is described as follows:

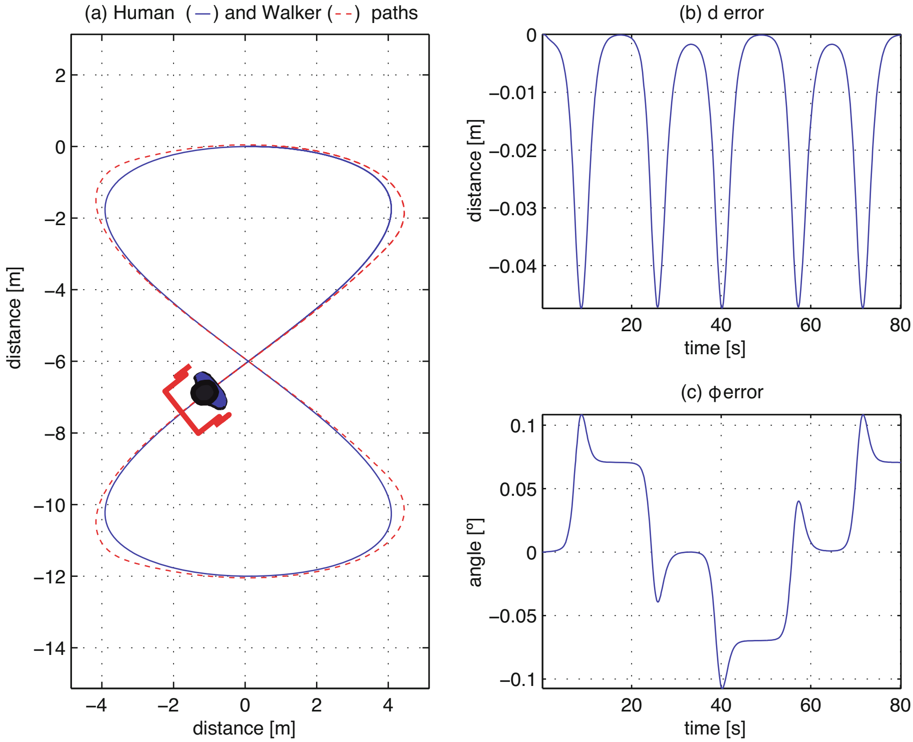

Fig. 10. Simulation of the proposed control strategy

θ and d. These parameters are measured directly using the LRF sensor after the legs detection process is performed. The leg detection algorithm consists of four steps. First, the area of interaction is reduced (in distance and aperture angle) to avoid the detection of legs of other individuals that are not driving the device. Note that the LRF can measure up to $4m$ of distance and 240 deg of aperture. Second, transitions in the distance vector are found to identify possible leg candidates. The third step is to use the transitions to classify the data into possible leg postures (separate, overlapped or together). Transitions that do not fulfill width and separation criteria are discarded. Finally, the coordinates of right and left legs are obtained. θ and d are obtained directly by averaging the left and right legs' coordinates.

v_h. The human linear velocity is obtained through the product of gait cadence ($steps/s$) and step amplitude ($m/step$). For that purpose, LDD, defined as the difference between the distances of left and right legs to the walker is fed into an adaptive filtering architecture. The filtering architecture that offers a real-time estimation of cadence and step amplitude will be addressed in the next section of this chapter

ω_h *and* ψ_h. Human angular velocity and orientation are obtained from the IMU placed on the human pelvis. The gyroscope integrated on the IMU offers a direct measurement of ω_h. ψ_h is obtained after the IMU orientation algorithm is performed [41]. In the same manner as previously performed to the force signals, cadence related components are also filtered using the Fourier Linear Combiner algorithm, canceling the influence of pelvic rotations during gait, and offering a more stable measurement of ψ_h.

ψ_w. Walker orientation is measured by the onboard IMU using the same IMU orientation algorithm [41].

ϕ. This angle represents the orientation difference between v_h and segment $\overline{WH}$. Fig. 9 shows that $\phi = \theta + \psi_h - \psi_w$. Also, ϕ is only defined if the magnitude of v_h is greater than zero.

Adaptive Estimation of Human Linear Velocity. As previously discussed, human linear velocity is obtained through the product of gait cadence and step amplitude. LDD, previously defined as the difference between the distances of left and right legs, can be used to obtain both parameters as it is shown in this section (Fig. 11).

The gait cadence can be defined as the rhythm of a person's walk, usually expressed in steps per minute (steps/min) [42]. This way, the frequency of the LDD signal yields cadence information. Additionally, the amplitude of the LDD signal (Fig. 11 a and b) is a direct measurement of the user's step length.

Considering the oscillatory nature of gait, a Weighted-Fequency Fourier Linear Combiner (WFLC) algorithm was proposed to obtain the frequency of LDD and, thus, the gait cadence. This information was also used as the gait cadence input to the controller presented in Section 3.1 (Fig. 6).

The WFLC is an extension of the FLC noise canceler, previously presented, that also tracks the frequency of an input signal based on a least-mean-square (LMS) recursion, a descend method based on a special estimate of the gradient [39]. Thus, it adapts, in real-time, its amplitude, frequency and phase to the reference signal [43]. The algorithm is based on a standard for fitting sine waves to noisy discrete-time observations, IEEE-STD-1057. The LMS recursion ensures inherent zero phase, thus allowing for real-time implementation.

The WFLC recursion minimizes the error ε_k between the input s_k and the signal harmonic model, as presented in (21). It assumes that the distance signal (LDD) can be mathematically modeled as a pure sinusoidal signal of frequency ω_{0_k} plus M harmonics [44].

$$\varepsilon_k = s_k - \sum_{r=1}^{M} \left[w_{r_k} \sin\left(r\omega_{0_k} k\right) + w_{r+M\,k} \cos\left(r\omega_{0_k} k\right) \right] \tag{21}$$

The WFLC provides an estimate of instantaneous frequency, as shown in (23).

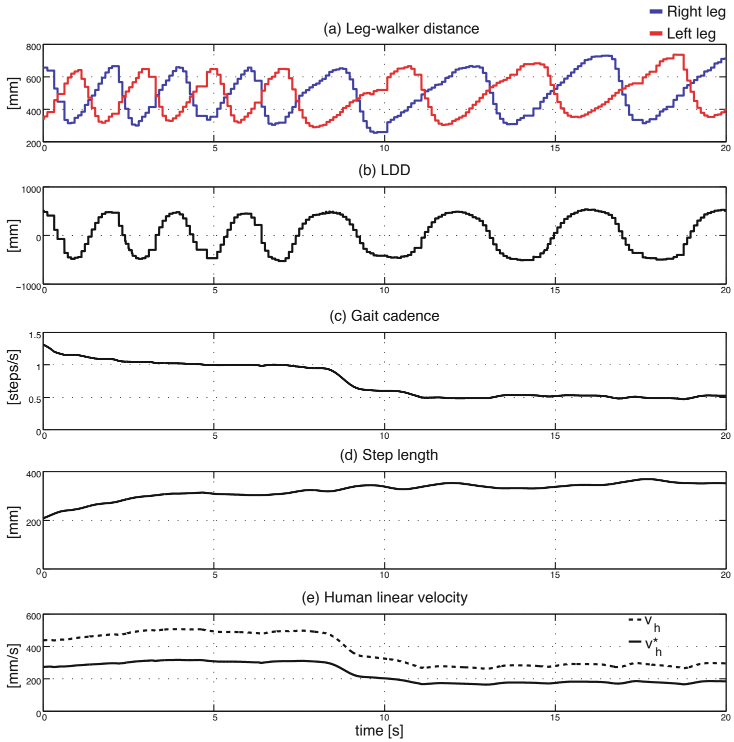

Fig. 11. (a) Leg to walker distances; (b) LDD signal obtained from the leg distances; (c) estimated gait cadence; (d) estimated step length; (e) human linear velocity obtained from the estimation of cadence and step length

$$\omega_{0_{k+1}} = \omega_{0_k} - 2\mu\varepsilon_k \frac{\partial \varepsilon_k}{\partial \omega_{0_k}} \tag{22}$$

$$\frac{\partial \varepsilon_k}{\partial \omega_{0_k}} = - k \sum_{k=1}^{M} \left[w_{r_k} \cos\left(r \sum_{t=1}^{k} \omega_{0_t} \right) - w_{r_k+M} \sin\left(r \sum_{t=1}^{k} \omega_{0_t} \right) \right] \tag{23}$$

The WFLC is formulated as follows:

– Equation (24) represents the sinusoidal signal model, which consists of M harmonics of the fundamental frequency, ω_{0_t}.
– Equation (25) describes the error which the algorithm uses to adapt itself to the input signal.
– Equations (26) and (27) express, respectively, the frequency and amplitude weights update based on the LMS algorithm [39].

$$x_{r_k} = \begin{cases} \sin\left(r \sum_{t=1}^{k} \omega_{0_t}\right), & 1 \leq r \leq M \\ \cos\left((r-M) \sum_{t=1}^{k} \omega_{0_t}\right), & M+1 \leq r \leq 2M \end{cases} \tag{24}$$

$$\varepsilon_k = s_k - \mathbf{W}_k^{\mathrm{T}} \mathbf{X}_k - \mu_b \tag{25}$$

$$\omega_{0_{k+1}} = \omega_{0_k} + 2\mu_0 \varepsilon_k \sum_{r=1}^{M} r\left(w_{r_k} x_{M+r_k} - w_{M+r_k} x_{r_k}\right) \tag{26}$$

$$\mathbf{W}_{k+1} = \mathbf{W}_k + 2\mu_1 \varepsilon_k \mathbf{X}_k \tag{27}$$

The algorithm has 5 parameters to be tuned [45]. M is the number of harmonics of the model which is fixed to 1. The instantaneous frequency at initialization is represented by $\omega_{0,0}$. Amplitude and frequency update weights are expressed by μ_0 and μ_1. Finally, μ_b is used to to compensate for low frequency drifts (bias weight).

As the WLFC is designed to adapt to the dominant-frequency component in a signal [46], it is important to perform a previous stage of band-pass filtering (compatible with gait cadence frequencies) for the correct performance of the WFLC (see Fig. 11 *c*). The band-pass filtering allows the WFLC to robustly adapt to the values of gait cadence.

Although this filtering stage can cause undesirable time delay in the filtered signals, here the WFLC algorithm is used only for cadence estimation. Considering the acquisition frequency, instantaneous temporal changes in gait cadence (WFLC's frequency output) are minimal, not affecting the performance of the proposed method. For amplitude estimation of the LDD signal, a FLC branch is used, operating on the raw input (Fig. 12), ensuring zero-phase amplitude estimation (see Fig. 11 *d*). Thus, the combination of WLFC and FLC presents great advantages [44].

Finally, as the LRF sensor is placed on a plane above the ground to allow robust detection of the users legs, a simple correction factor is applied to the signal $v_h = k * v_h^*$. Fig. 11 *e* shows the human linear velocity calculated by the product of *gait cadence* and *step length* before and after the correction factor is applied (solid and dashed line, respectively). Notice that in this sample experiment, the user was asked to walk at $500mm/s$ on the first half of the experiment and, then, slow down to $250mm/s$. Gait speed was indicated to the user by ground marks (to ensure step length) and a metronome (for indicating cadence). Step lengths were maintained constant at $500mm$ as gait cadence varied from 1 $step/s$ to 0.5 $step/s$.

Results and Discussion. The inverse kinematic interaction strategy proposed in this section was validated in the Intelligent Automation Laboratory (LAI) at Federal University of Espirito Santo, Brazil. Considering that the proposed controller relies only on LRF and IMU information, this stage of validation required no physical contact between user and walker. Based on this requirement, no experiments could be performed with patients suffering from gait disorders, as physical support would be required to assist gait.

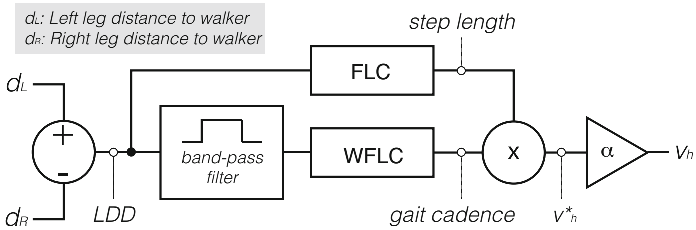

Fig. 12. Adaptive estimation architecture to obtain human linear velocity

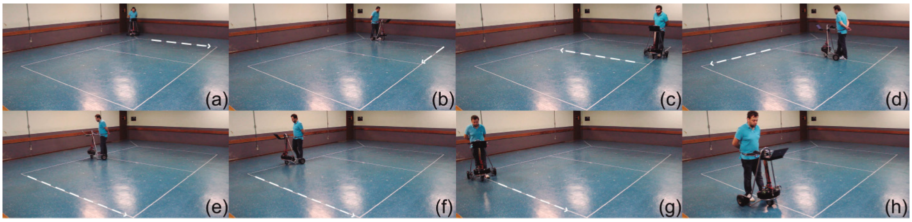

Fig. 13. 8-shaped path performed on the validation experiments

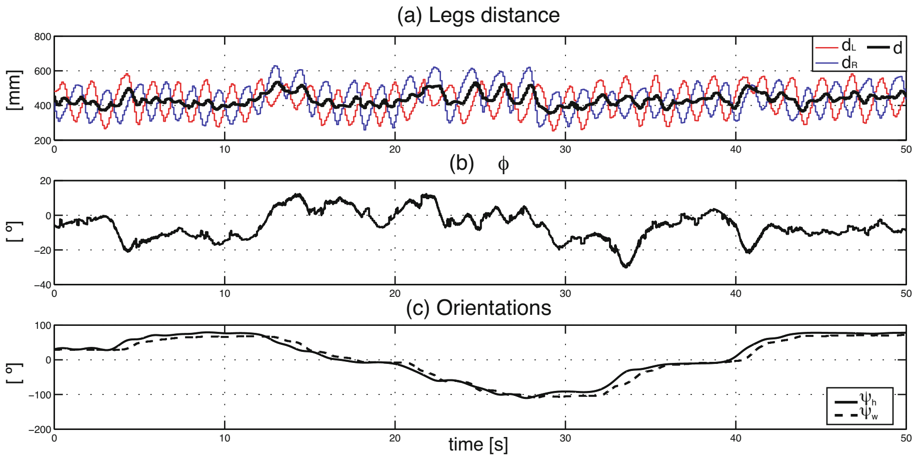

Fig. 14. Data obtained from a sample experiment: (a)The leg detection algorithm outputs (d_L and d_R) and user-walker distance d; (b) ϕ angle; and (c) user and walker orientation angles

A sample experiment of an 8-shaped path performed during the validation experiments with healthy subjects is presented in Fig. 13. It is possible to observe that the user keeps his upper-limbs behind his back at all moments, avoiding any physical interaction with the device.

Fig. 14 shows the results of a sample experiment. The leg detection algorithm outputs (d_L and d_R) are presented in Fig. 14 *a*. The user-walker distance (d) is obtained by averaging d_L and d_R. The control law aims to achieve a desired human-walker distance ($500mm$ in this experiment) and an ϕ angle equals to zero. The ϕ angle is presented in Fig. 14 *b*. Finally, user and walker orientation angles are also presented to illustrate that the robotic walker is always correctly orientated to the user during the performed 8-shaped path.

4 Conclusions and Future Work

This chapter presented the robotic walker developed at the Federal University of Espirito Santo (UFES), Brazil. After a brief description of the general concepts involved in locomotion, mobility dysfunctions and assistive devices, a functional classification of the Smart Walkers was presented.

The UFES Smart Walker was introduced as a system focused on user-machine multimodal interaction for obtaining a natural control strategy for the robotic device. Past experiences and current developments were addressed, especially considering interaction and control strategies to drive the robotic device. First, an adaptive filtering strategy of the upper-body interaction forces was presented. In this case, a Fuzzy-Logic based control system was developed to generate the navigation commands to the device.

A second approach based on a robust inverse kinematics controller was introduced in section 3.2. The navigation commands were obtained from the user's motions obtained by a laser range finder and a wearable inertial measurement unit, also developed at UFES, Brazil.

Currently, the authors are working on the fusion of both control methods aiming at obtaining a robust and safe interaction strategy to assist patients suffering from locomotion disorders. Once a reliable fusion strategy is conceived, the device will be validated with osteoarthritis and cerebrovascular accident (CVA) patients at the Center of Physical Rehabilitation of Espirito Santo (CREFES), Brazil.

Acknowledgments. This research is supported by the Brazilian National Council for Scientific and Technological Development (CNPq), Process # 471804/2012-6.

References

1. Winter, D.: Biomechanics and motor control of human movement. John Wiley & Sons (2009)
2. Buchman, A., Boyle, P., Leurgans, S., Barnes, L., Bennet, D.: Cognitive function is associated with the development of mobility impairments in community-dwelling elders. The American Journal of Geriatric Psychiatry 19(6), 571–580 (2011)
3. Van Hook, F.W., Demonbreun, D., Weiss, B.D.: Ambulatory devices for chronic gait disorders in the elderly. American Family Physician 67(8), 1717–1724 (2003)

4. Lam, R.: Practice tips: choosing the correct walking aid for patients. Canadian Family Physician Médecin de Famille Canadien 53(12), 2115–2116 (2007)
5. Ceres, R., Pons, J., Calderón, L., Mesonero-Romanos, A., Jiménez, A., Sánchez, F., Abizanda, P., Saro, B., Bonivardo, G.: Andador activo para la rehabilitación y el mantenimiento de la movilidad natural. In: IMSERSO, pp. 3–8 (2004)
6. Gross, K.D.: Device use: walking AIDS, braces, and orthoses for symptomatic knee osteoarthritis. Clinics in Geriatric Medicine 26(3), 479–502 (2010)
7. Bateni, H., Maki, B.E.: Assistive Devices for Balance and Mobility: Benefits, Demands, and Adverse Consequences. Archives of Physical Medicine and Rehabilitation 86(1), 134–145 (2005)
8. Haubert, L.L., Gutierrez, D.D., Newsam, C.J., Gronley, J.K., Mulroy, S.J., Perry, J.: A comparison of shoulder joint forces during ambulation with crutches versus a walker in persons with incomplete spinal cord injury. Archives of Physical Medicine and Rehabilitation 87(1), 63–70 (2006)
9. Priebe, J.R., Kram, R.: Why is walker-assisted gait metabolically expensive? Gait & Posture 34(2), 265–269 (2011)
10. Frizera, A., Ceres, R., Pons, J.L., Abellanas, A., Raya, R.: The Smart Walkers as Geriatric Assistive Device. The SIMBIOSIS Purpose. In: Proceedings of the 6th International Conference of the International Society for Gerontechnology, pp. 1–6 (2008)
11. Elias, A., Frizera, A., Bastos, T.: Robotic walkers from a clinical point of view: feature-based classification and proposal of a model for rehabilitation programs. In: XIV Reunión de Trabajo en Procesamiento de la Información y Control, pp. 1–5 (2011)
12. Yu, H., Spenko, M., Dubowsky, S.: Omni-Directional Mobility Using Active Split Offset Castors. Journal of Mechanical Design 126(5), 822 (2004)
13. MacNamara, S., Lacey, G.: A smart walker for the frail visually impaired. In: Proceedings 2000 ICRA. Millennium Conference. IEEE International Conference on Robotics and Automation. Symposia Proceedings, pp. 1354–1359. IEEE (2000)
14. Hirata, Y., Muraki, A., Kosuge, K.: Motion control of intelligent passive-type Walker for fall-prevention function based on estimation of user state. In: Proceedings of IEEE International Conference on Robotics and Automation, ICRA 2006, pp. 3498–3503 (May 2006)
15. Hirata, Y., Muraki, A., Kosuge, K.: Standing Up and Sitting Down Support Using Intelligent Walker Based on Estimation of User States. In: 2006 International Conference on Mechatronics and Automation, pp. 13–18. IEEE (June 2006)
16. Morris, A., Donamukkalat, R., Kapuria, A., Steinfeldt, A., Matthews, J.T., Dunbar-Jacob, J., Thrunti, S.: A Robotic Walker That Provides Guidance. In: Proceedings of the 2003 IEEE lnternational Conference on Robotics & Automation, pp. 25–30 (2003)
17. Rentschler, A.J., Cooper, R.A., Blasch, B., Boninger, M.L.: Intelligent walkers for the elderly: performance and safety testing of VA-PAMAID robotic walker. Journal of Rehabilitation Research and Development 40(5), 423–431 (2003)
18. Chugo, D., Asawa, T., Kitamura, T., Takase, K.: A moving control of a robotic walker for standing, walking and seating assistance. In: 2008 IEEE International Conference on Robotics and Biomimetics, pp. 692–697. IEEE (February 2008)
19. Chugo, D., Kitamura, T., Takase, K.: A rehabilitation walker with standing and walking assistance. In: 2008 IEEE/RSJ International Conference on Intelligent Robots and Systems, pp. 260–265. IEEE (September 2008)

20. Médéric, P., Pasqui, V., Plumet, F., Bidaud, P.: Design of a walking-aid and sit to stand transfer assisting device for elderly people 2 Disturbances induced by some particular. In: Proceedings of ROMAN 2004-15th CISM-IFToMM Symposium on Robot Design, Dynamics and Control, pp. 5–12 (2004)
21. Abellanas, A., Frizera, A., Ceres, R., Raya, R.: Assessment of the laterality effects through forearm reaction forces in walker assisted gait. Procedia Chemistry 1(1), 1227–1230 (2009)
22. Lacey, G., Namara, S.M., Dawson-Howe, K.M.: Personal adaptive mobility aid for the infirm and elderly blind. In: Mittal, V.O., Yanco, H.A., Aronis, J., Simpson, R.C. (eds.) Assistive Technology and AI. LNCS (LNAI), vol. 1458, pp. 211–220. Springer, Heidelberg (1998)
23. Rodriguez-Losada, D., Matia, F., Jimenez, A., Lacey, G.: Guido, the Robotic SmartWalker for the frail visually impaired. In: First International Conference on Domotics, Robotics and Remote Assitence for All - DRT4all, pp. 1–14 (2005)
24. Graf, B.: An Adaptive Guidance System for Robotic Walking Aids. Journal of Computing and Information Technology 1(1), 109–120 (2008)
25. Kulyukin, V., Kutiyanawala, A., LoPresti, E., Matthews, J., Simpson, R.: iWalker: Toward a Rollator-Mounted Wayfinding System for the Elderly. In: 2008 IEEE International Conference on RFID, pp. 303–311 (April 2008)
26. Zong, C., Chetouani, M., Tapus, A.: Automatic gait characterization for a mobility assistance system. In: 11th International Conference in Control, Automation, Robotics and Vision, pp. 473–478 (2010)
27. Chan, A.D.C., Green, J.R.: Smart Rollator Prototype. In: 2008 IEEE International Workshop on Medical Measurements and Applications, pp. 97–100. IEEE (May 2008)
28. Alwan, M., Wasson, G., Sheth, P., Ledoux, A., Huang, C.: Passive derivation of basic walker-assisted gait characteristics from measured forces and moments. In: Conference Proceedings: ... Annual International Conference of the IEEE Engineering in Medicine and Biology Society. IEEE Engineering in Medicine and Biology Society, vol. 4, pp. 2691–2694 (January 2004)
29. Dubowsky, S., Genot, F., Godding, S., Kozono, H., Skwersky, A., Yu, H., Yu, L.S.: PAMM - A Robotic Aid to the Elderly for Mobility Assistance and Monitoring: A "Helping-Hand" for the Elderly. In: Proceedings of the IEEE Conference on Robotics and Automation - ICRA (2000)
30. Henry, J., Aharonson, V.: Gait monitoring for the elderly using a robotic walking aid. In: IEEE 26th Convention of Electrical and Electronics Engineers in Israel, pp. 392–394 (2010)
31. Spenko, M., Yu, H., Dubowsky, S.: Robotic personal aids for mobility and monitoring for the elderly. IEEE Transactions on Neural Systems and Rehabilitation Engineering: A Publication of the IEEE Engineering in Medicine and Biology Society 14(3), 344–351 (2006)
32. Frizera, A., Cifuentes, C.A., Bastos, T.F.: Motion Capture System Based on the Integration of 3D Accelerometer in a Wireless Inertial Measurement Unit. In: Accelerometers: Principles, Structure and Applications, vol. 1, pp. 57–76. Nova Science Publishers, Inc. (2013)
33. Frizera, A., Ceres, R., Rocon, E., Pons, J.L.: Empowering and Assisting Natural Human Mobility: The Simbiosis Walker 8(3), 34–50 (2011)
34. Abellanas, A., Frizera, A., Ceres, R., Gallego, J.: Estimation of gait parameters by measuring upper limb-walker interaction forces. Sensors and Actuators A: Physical 162(2), 276–283 (2010)

35. Frizera Neto, A., Gallego, J.A., Rocon, E., Pons, J.L., Ceres, R.: Extraction of user's navigation commands from upper body force interaction in walker assisted gait. BioMedical Engineering Online 9(37), 1–16 (2010)
36. Brookner, E.: Tracking and Kalman Filtering Made Easy. John Wiley and Sons, Inc. (1998)
37. Mann, K., Werner, F.W., Palmer, A.K.: Frequency spectrum analysis of wrist motion for activities of daily living. Journal of Orthopedic Research 7(2), 304–306 (1989)
38. Benedict, T.R., Bordner, G.: Synthesis of an optimnal set of radar track-while-scan smoothing equations. IRE Transactions on Automatic Control 7(4), 27–32 (1962)
39. Widrow, B., Stearns, S.D.: Adaptive signal processing. Prentice Hall (1985)
40. Frizera, A.: Interfaz multimodal para modelado, estudio y asistencia a la marcha humana mediante andadores robóticos. PhD thesis, Universidad de Alcalá (2010)
41. Braidot, A., Cifuentes, C., Frizera Neto, A., Frisoli, M., Santiago, A.: Zigbee wearable sensor development for upper limb robotics rehabilitation. Latin America Transactions, IEEE (Revista IEEE America Latina) 11(1), 408–413 (2013)
42. Frizera, A., Elias, A., del Ama, A., Ceres, R., Bastos, T.: Characterization of spatiotemporal parameters of human gait assisted by a robotic walker. In: 2012 4th IEEE RAS EMBS International Conference on Biomedical Robotics and Biomechatronics (BioRob), pp. 1087–1091 (2012)
43. Riviere, C.N., Rader, R.S., Thakor, N.V.: Adaptive canceling of physiological tremor for improved precision in microsurgery. IEEE Transactions on Biomedical Engineering 45(7), 839–846 (1998)
44. Riviere, C., Khosla, P.: Augmenting the human-machine interface: improving manual accuracy. In: IEEE International Conference on Robotics and Automation, vol. 4, pp. 3546–3550 (1997)
45. Riviere, C.: Adaptive suppression of tremor for improved human-machine control. PhD thesis, Johns Hopkins University (1995)
46. Riviere, C.N., Thakor, N.V.: Modeling and canceling tremor in human-machine interfaces. IEEE Engineering in Medicine and Biology 15(3), 29–36 (1996)